Journal of Applied Fluid Mechanics, Vol. 11, No. 4, pp. 1047-1057, 2018.
Available online at www.jafmonline.net, ISSN 1735-3572, EISSN 1735-3645.
DOI: 10.29252/jafm.11.04.27914

Wave Motion due to a Ring Source in Two Superposed Fluids Covered by a Thin Elastic Plate

N. Islam[1], R. Gayen[1†], and B. N. Mandal[2]

[1] *Department of Mathematics, Indian Institute of Technology, Kharagpur - 721302, India*
[2] *Physics and Applied Mathematics Unit, Indian Statistical Institute, Kolkata 700108, India*

† *Corresponding Author Email: rupanwita.gayen@gmail.com*

(Received April 25, 2017; accepted January 9, 2018)

ABSTRACT

The problem of wave generation by a horizontal ring of wave sources of the same time-dependent strength present in any one layer of a two-layer fluid is investigated here. The upper fluid is of finite height above the interface and is covered by a floating thin infinite elastic plate (modeling a thin sheet of ice) while the lower fluid extends infinitely downwards. Assuming linear theory, the problem is formulated as an initial value problem and the Laplace transform in time is employed to solve it. For time-harmonic source strength, the asymptotic representations of the potential functions describing the motion in the two layers for large time and distance are derived. In these representations, the two different coefficients for each of the surface and interface wave modes have the same numerical values although it has not been possible to prove their equivalence analytically. This shows that the steady-state analysis of the potential functions produces outgoing progressive waves at the surface and at the interface. The forms of the surface and interface waves are depicted graphically for different values of the flexural rigidity of the elastic plate and the ring source being submerged in the lower or upper layer.

Keywords: Ring source potentials; Two-layer fluid; Thin elastic plate; Steady-state analysis.

1. INTRODUCTION

Investigation of wave problems in water covered by a thin sheet of ice modeled as a thin elastic plate has gained considerable importance due to two reasons. One is due to investigation of the mechanism and effects of wave propagation through Marginal Ice Zone in polar regions while the other is due to their applications in the construction of Very Large Floating Structures like oil storage bases, off-shore pleasure cities, floating airport runways etc. In a single-layer fluid, significant ice-wave interaction problems were considered by Fox and Squire (1994), Squire and Williams (2008), Feng and Lu (2009) and others. During winter the Norwegian fjords consisting of a layer of fresh water on the top of a very deep layer of salt water are covered by an ice sheet and thus a two-layer fluid where the upper layer has an ice-cover becomes a reality. A number of researchers investigated ice-wave interaction problems in a two-layer fluid. For example Das and Mandal (2007), Mohapatra and Bora (2012), Panda and Martha (2013) and others have analyzed various types of water wave problems in a two-layer fluid when the upper layer is covered by a thin sheet of ice modeled as an elastic plate.

There has been a long standing interest in studying water wave generation problems by various disturbances present either on the surface or inside the water. If a body or a number of bodies are present in water, waves may be either generated by the movement of the body, or reflected from the body. The two cases are identical, and the resulting motion in the fluid can be described by a series of singularities placed on the surface of the body or bodies. These singularities are characterized by their giving rise to potentials which are typical singular solutions of Laplace's equation in the neighborhood of the singularity. For the two-dimensional case these singularities are either of logarithmic type or of multipole type, and for the three-dimensional case these are point sources or point multipoles. Many authors have investigated different types of singularities that can be used in single-fluid problems. Thorne (1953), Chowdhury and Mandal (2006), Lu and Dai (2008) gave surveys of the fundamental line and point singularities submerged in a single-fluid of finite or infinite depth. Analysis of fluid motion due to various types of singularities present in a two-fluid medium can be found in Gorgui and Kassem (1978), Yeung and Nguyen (1999), Ten and Kashiwagi (2004), Manyanga and Duan (2011) and others.

If an obstacle is in the form of a vertical body of revolution having a common vertical axis of symmetry with the fluid motion, one needs to consider potential due to submerged horizontal circular rings of wave sources since the problem can then be formulated in terms of suitable distribution of rings of wave sources around the body. An offshore structure in the high sea for the purpose of oil prospecting may be modeled as a vertical cylinder of circular cross section. Hence consideration of velocity potentials due to submerged circular rings of wave sources is of importance (cf. Fenton (1978), Hulme (1981)). Rhodes-Robinson (1984), Mandal and Kundu (1987), Chowdhury and Mandal (2004) and others have investigated the problems of wave motion generated due to the presence of a ring source placed in a single-layer fluid when the upper surface is free or covered by an inertial surface or thin ice sheet modeled as a thin elastic plate. Problems dealing with the generation of internal waves at the surface separating two fluids due to the presence of a vertical body of revolution present in either of the fluids can be formulated in terms of a suitable distribution of ring of wave sources around the body as is done for a single fluid. Mandal and Kundu (1988) used Laplace transform technique to obtain the velocity potential due to a ring source of time-dependent strength submerged in one of the fluids of a two-fluid medium when the upper fluid extends infinitely upwards, while the lower fluid is of finite constant depth and the two-fluid medium separated by an inertial surface composed of a thin uniform distribution of disconnected materials. Mandal and Chakrabarti (1995) investigated the problem of wave motions generated due to the presence of a ring source placed in either of the fluids of a two-fluid medium when the upper fluid is of finite height above the mean interface and bounded by a free surface while the lower fluid extend infinitely downwards.

Here we consider the motion due to a horizontal ring of wave sources of time-dependent strength present in either of the fluids of a two-fluid medium when the upper fluid is of finite height above the mean interface and bounded by a thin elastic sheet modeling a thin sheet of ice, while the lower layer extends infinitely downwards. The problem is formulated as an initial value problem for the velocity potentials describing the motion in the fluids and Laplace transform in time is employed to solve it. After invoking the inverse transform, the potential functions are obtained and then their asymptotic representations for large time and large distance are derived. The derivation is carried out separately for the cases when the ring source is placed in the lower layer and also when it is placed in the upper layer. In the asymptotic representations, the two different coefficients each for surface and interface wave mode produce almost the same numerical results although it has not been possible to prove their equivalence analytically. This shows that the steady-state analysis of the potentials produces the existence of outgoing progressive waves at the surface and the interface. The surface and interface wave profiles are depicted graphically in a number of figures for different values of the flexural rigidity of the elastic plate and the ring source being submerged in the lower or upper fluid.

2. MATHEMATICAL FORMULATION

We consider the irrotational motion of two inviscid incompressible fluids with ρ_1 and ρ_2 ($< \rho_1$) as the densities of the lower and upper fluids respectively. The upper fluid is of finite depth h and covered by a thin uniform ice sheet modeled as a thin elastic plate, while the lower fluid is infinitely deep. Here we use a cylindrical coordinate system (R,θ,y) in which the y-axis is taken vertically downwards passing through the center of the horizontal ring of radius a of uniformly distributed line sources each of strength $m(t)$ submerged in either of the fluids at a depth η below the undisturbed floating thin elastic plate. Since the strength $m(t)$ does not depend on θ, the motion of the fluid is axisymmetric. The plane $y = 0$ denotes the rest position of the thin elastic plate and the common interface of the two fluids is represented by the horizontal plane $y = h$. We assume the motion to start from rest at the instant when the sources on the ring simultaneously start operating. Thus the motion is irrotational and can be described by potential functions $\phi_j^{(i)}(R,y,t)$, where the subscripts $j = 1,2$ refer to the lower and upper fluids respectively, $i = 1,2$ are taken for the cases of ring sources submerged in lower and upper fluids respectively. Then $\phi_j^{(i)}$'S$(j=1,2)$ satisfy the Laplace's equation

$$\left\{\mathcal{L}\left(R,\frac{\partial}{\partial R}\right)+\frac{\partial^2}{\partial y^2}\right\}\phi_j^{(i)}=0 \tag{1}$$

except at points on the ring, where $\mathcal{L}\left(R,\frac{\partial}{\partial R}\right)=\frac{\partial^2}{\partial R^2}+\frac{1}{R}\frac{\partial}{\partial R}$.

If $\zeta_2^{(i)}(R,t)$ denotes the depression of the upper surface below its mean position, then the linearized kinematic and dynamic boundary conditions on upper surface are given by:

$$\frac{\partial \phi_2^{(i)}}{\partial y}=\frac{\partial \zeta_2^{(i)}}{\partial t} \quad \text{on } y=0, \tag{2}$$

$$\frac{\partial}{\partial t}\left(\phi_2^{(i)}-\varepsilon\frac{\partial \phi_2^{(i)}}{\partial y}\right)=\left\{D\mathcal{L}^2\left(R,\frac{\partial}{\partial R}\right)+1\right\}g\zeta_2^{(i)} \tag{3}$$

on $y = 0$.

Here $D=\frac{L}{\rho_2 g}$ and $\varepsilon=\frac{\rho}{\rho_2}h_1$, $L=\frac{Eh_1^3}{12\left(1-\nu^2\right)}$

being the flexural rigidity of the ice-sheet, h_l being the very small thickness of the elastic plate, ρ being the density of the ice, E and v being the Young's modulus and Poisson's ratio of the material of the elastic plate respectively.

Eliminating $\zeta_2^{(i)}$ between (2) and (3), we obtain the boundary condition on the elastic plate as

$$\frac{\partial^2}{\partial t^2}\left(\phi_2^{(i)}-\varepsilon\frac{\partial\phi_2^{(i)}}{\partial y}\right)=\left\{D\mathcal{L}^2\left(R,\frac{\partial}{\partial R}\right)+1\right\}g\frac{\partial\phi_2^{(i)}}{\partial y} \tag{4}$$

on y= 0.

If $\zeta_1^{(i)}(R,t)$ denotes the interface surface depression below the mean position, then the linearized kinematic and dynamic boundary conditions at the interface are given by the following equations:

$$\frac{\partial\phi_2^{(i)}}{\partial y}=\frac{\partial\phi_1^{(i)}}{\partial y}=\frac{\partial\zeta_1^{(i)}}{\partial t}\ \text{on}\ y=h, \tag{5}$$

$$s\left(\frac{\partial\phi_2^{(i)}}{\partial t}-g\zeta_1^{(i)}\right)=\frac{\partial\phi_1^{(i)}}{\partial t}-g\zeta_1^{(i)}\ \text{on}\ y=h, \tag{6}$$

where $s=\frac{\rho_2}{\rho_1}$.

Eliminating $\zeta_1^{(i)}$ between (5) and (6), we obtain the interface boundary condition as

$$\frac{\partial^2}{\partial t^2}\left(s\phi_2^{(i)}-\phi_1^{(i)}\right)=g\frac{\partial}{\partial y}\left(s\phi_2^{(i)}-\phi_1^{(i)}\right)\ \text{on}\ y=h. \tag{7}$$

Also condition at large depth is

$$\nabla\phi_1^{(i)}\to 0\ \text{as}\ y\to\infty. \tag{8}$$

At points near the ring

$$\phi\to m(t)\phi_0\ \ as\ \sqrt{(R-a)^2+(y-\eta)^2}\to 0 \tag{9}$$

where ϕ is $\phi_1^{(1)}$ if the ring is in the lower fluid while ϕ is $\phi_2^{(2)}$ if the ring is in the upper fluid and ϕ_0 is the potential due to a ring of wave sources of constant unit strength in an unbounded fluid, given by (cf. Hulme (1981))

$$\phi_0=2\pi a\int_0^\infty e^{-k|y-\eta|}J_0(ka)J_0(kR)dk. \tag{10}$$

3. SOLUTIONS TO THE PROBLEMS

In order to solve the boundary value problem given by Eqs. (1), (4), (5) and (7) − (9), we employ the Laplace transform technique. Let $\Phi_j^{(i)}(R,y,p)$ denote the Laplace transform of $\phi_j^{(i)}(R,y,t)$ defined as

$$\Phi_j^{(i)}(R,y,p)=\int_0^\infty\phi_j^{(i)}(R,y,t)e^{-pt}dt\ \ (p>0), \tag{11}$$

then $\Phi_j^{(i)}$'s satisfy the BVP described by

$$\left\{\mathcal{L}\left(R,\frac{\partial}{\partial R}\right)+\frac{\partial^2}{\partial y^2}\right\}\Phi_j^{(i)}=0, \tag{12}$$

except at points on the ring,

$$p^2\Phi_2^{(i)}=\left\{D\mathcal{L}^2\left(R,\frac{\partial}{\partial R}\right)+1+\frac{\varepsilon p^2}{g}\right\}g\frac{\partial\Phi_2^{(i)}}{\partial y} \tag{13}$$

on $y=0$,

$$\frac{\partial\Phi_2^{(i)}}{\partial y}=\frac{\partial\Phi_1^{(i)}}{\partial y}\ \ on\ \ y=h, \tag{14}$$

$$s\left(p^2\Phi_2^{(i)}-g\frac{\partial\Phi_2^{(i)}}{\partial y}\right)=\left(p^2\Phi_1^{(i)}-g\frac{\partial\Phi_1^{(i)}}{\partial y}\right) \tag{15}$$

on $y=h$,

$$\nabla\Phi_1^{(i)}\to 0\ \ as\ \ y\to\infty, \tag{16}$$

$$\Phi\to M(p)\phi_0\ \ as\ \sqrt{(R-a)^2+(y-\eta)^2}\to 0 \tag{17}$$

where Φ is $\Phi_1^{(1)}$ if the ring is in the lower fluid while Φ is $\Phi_2^{(2)}$ if the ring is in the upper fluid and $M(p)$ is the Laplace transform of $m(t)$.

4. RING SOURCE SUBMERGED IN LOWER FLUID

We first assume that the ring source is submerged in the lower fluid and solve the boundary value problem governed by the Eqs. (12)-(17). For this we represent $\Phi_j^{(1)}(R,y,p)$'s $(j=1,2)$ as

$$\begin{aligned}\Phi_1^{(1)}(R,y,p)&=M(p)\left[\phi_0-2\pi a\int_0^\infty e^{-k(y+\eta)}J_0(ka)J_0(kR)dk\right]\\&+\int_0^\infty A_1^{(1)}(k)e^{-k(y-h)}J_0(ka)J_0(kR)dk.\end{aligned} \tag{18}$$

$$\begin{aligned}\Phi_2^{(1)}(R,y,p)=\int_0^\infty\Big\{&B_2^{(1)}(k)\cosh k(h-y)\\&+C_2^{(1)}(k)\sinh ky\Big\}\frac{J_0(ka)}{\cosh kh}J_0(kR)dk.\end{aligned} \tag{19}$$

Here $A_1^{(1)}(k), B_2^{(1)}(k), C_2^{(1)}(k)$ are unknown functions and are determined by using the conditions (13) − (15).

The final results after rearrangement take the forms

$$\Phi_1^{(1)} = M(p)\Big[U_1^{(1)}(R,y) + 4\pi a\int_0^\infty a_1(k)E(k) \times\left\{\frac{F(\rho_1,\rho_2,\alpha)}{p^2+\alpha^2} - \frac{F(\rho_1,\rho_2,\beta)}{p^2+\beta^2}\right\} \times \cosh kh e^{-k(y+\eta-h)} J_0(ka)J_0(kR)dk\Big], \quad (20)$$

$$\Phi_2^{(1)} = M(p)\Big[U_2^{(1)}(R,y) + 4\pi a\int_0^\infty \varepsilon k E(k) \times\left\{\frac{F(\gamma_1,\gamma_2,\alpha)}{p^2+\alpha^2} - \frac{F(\gamma_1,\gamma_2,\beta)}{p^2+\beta^2}\right\} \times e^{k(h-\eta)}\cosh k(h-y) J_0(ka)J_0(kR)dk - 4\pi a\int_0^\infty a_1(k)E(k) \times\left\{\frac{F(\rho_1,\rho_2,\alpha)}{p^2+\alpha^2} - \frac{F(\rho_1,\rho_2,\beta)}{p^2+\beta^2}\right\} \times e^{-k\eta}\sinh ky J_0(ka)J_0(kR)dk\Big], \quad (21)$$

where

$$U_1^{(1)}(R,y) = 2\pi a\int_0^\infty\left\{e^{-k|y-\eta|} - e^{-k(y+\eta)}\right\} \times J_0(ka)J_0(kR)dk + 4\pi a\int_0^\infty \frac{a_1(k)}{m_1(k)} \times \cosh kh e^{-k(y+\eta-h)} J_0(ka)J_0(kR)dk,$$

$$U_2^{(1)}(R,y) = 4\pi a\int_0^\infty \frac{\varepsilon k}{m_1(k)} e^{k(h-\eta)}\cosh k(h-y) \times J_0(ka)J_0(kR)dk + 4\pi a\int_0^\infty\left(1-\frac{a_1(k)}{m_1(k)}\right) \times e^{-k\eta}\sinh ky J_0(ka)J_0(kR)dk,$$

$$a_1(k) = s\varepsilon k - (1-s)\Gamma_1(k)\sinh kh,$$

$$a_2(k) = b_1(k)\left\{s + (1-s)\sinh^2 kh\right\} + (1-s)gk\Gamma_1(k)\cosh kh,$$

$$b_1(k) = gk(Dk^4+1), \qquad \Gamma_1(k) = \cosh kh + \varepsilon k\sinh kh,$$

$$m_1(k) = \cosh kh\left\{s(\sinh kh + \varepsilon k\cosh kh) + \Gamma_1(k)\right\},$$

$$m_2(k) = \cosh kh\left\{b_1(k)(s\cosh kh + \sinh kh) + (1-s)gk\Gamma_1(k)\right\},$$

$$m_3(k) = (1-s)gkb_1(k)\sinh kh\cosh kh,$$

$$\alpha^2+\beta^2 = \frac{m_2}{m_1}, \qquad \alpha^2\beta^2 = \frac{m_3}{m_1}, \qquad \rho_1 = \frac{a_2m_1 - a_1m_2}{a_1m_1},$$

$$\rho_2 = \frac{m_3(a_1-m_1)}{a_1m_1}, \qquad \gamma_1 = \frac{b_1m_1 - \varepsilon km_2}{\varepsilon km_1}, \qquad \gamma_2 = \frac{m_3}{m_1},$$

$$E(k) = \frac{1}{m_1}\frac{1}{\alpha^2-\beta^2}, \qquad F(\tau_1,\tau_2,\nu) = \tau_1\nu^2 + \tau_2.$$

In order to obtain the velocity potentials $\phi_j^{(1)}$ we employ Laplace inversion of Eqs. (20) and (21). This gives

$$\phi_1^{(1)} = m(t)U_1^{(1)}(R,y) + 4\pi a\Big[\int_0^\infty a_1(k)E(k) \times\left\{F(\rho_1,\rho_2,\alpha)I(t,\alpha) - F(\rho_1,\rho_2,\beta)I(t,\beta)\right\} \times\cosh kh e^{-k(y+\eta-h)} J_0(ka)J_0(kR)dk\Big], \quad (22)$$

$$\phi_2^{(1)} = m(t)U_2^{(1)}(R,y) + 4\pi a\Big[\int_0^\infty \varepsilon kE(k) \times\left\{F(\gamma_1,\gamma_2,\alpha)I(t,\alpha) - F(\gamma_1,\gamma_2,\beta)I(t,\beta)\right\} \times e^{k(h-\eta)}\cosh k(h-y)J_0(ka)J_0(kR)dk\Big] - 4\pi a\Big[\int_0^\infty a_1(k)E(k)\left\{F(\rho_1,\rho_2,\alpha)I(t,\alpha) - F(\rho_1,\rho_2,\beta)I(t,\beta)\right\}e^{-k\eta}\sinh ky \times J_0(ka)J_0(kR)dk\Big], \quad (23)$$

where

$$I(t,\nu) = \frac{1}{\nu}\int_0^t \sin\nu(t-\tau)m(\tau)d\tau.$$

When the ring source is of time-harmonic strength, say $m(t) = \sin\sigma t,$ the potential functions $\phi_j^{(1)}$ have the following forms:

$$\phi_1^{(1)} = \sin\sigma t U_1^{(1)}(R,y) + 4\pi a\Big[\int_0^\infty a_1(k)E(k) \times\left\{F(\rho_1,\rho_2,\alpha)S(t,\alpha) - F(\rho_1,\rho_2,\beta)S(t,\beta)\right\} \times\cosh kh e^{-k(y+\eta-h)} J_0(ka)J_0(kR)dk\Big], \quad (24)$$

$$\phi_2^{(1)} = \sin\sigma t U_2^{(1)}(R,y) + 4\pi a\Big[\int_0^\infty \varepsilon kE(k) \times\left\{F(\gamma_1,\gamma_2,\alpha)S(t,\alpha) - F(\gamma_1,\gamma_2,\beta)S(t,\beta)\right\} \times e^{k(h-\eta)}\cosh k(h-y)J_0(ka)J_0(kR)dk\Big] - 4\pi a\Big[\int_0^\infty a_1(k)E(k)\left\{F(\rho_1,\rho_2,\alpha)S(t,\alpha) - F(\rho_1,\rho_2,\beta)S(t,\beta)\right\}e^{-k\eta}\sinh ky \times J_0(ka)J_0(kR)dk\Big], \quad (25)$$

where

$$S(t,\nu) = \frac{\nu\sin\sigma t - \sigma\sin\nu t}{\nu\left(\nu^2-\sigma^2\right)}.$$

To isolate the steady-state term and transient term in the Eqs. (24) and (25), we rewrite $\phi_j^{(1)}$ as

$$\phi_1^{(1)} = 2\pi a \sin\sigma t \int_0^\infty \left\{ W_1^{(1)}(k,y) - 2\frac{X_1^{(1)}(k,y)}{m_1(k)\Delta(k)} \right\} J_0(kR)dk - 4\pi a \int_0^\infty \sigma a_1(k)E(k) \times \left\{ F(\rho_1,\rho_2,\alpha)T(t,\alpha) - F(\rho_1,\rho_2,\beta)T(t,\beta) \right\} \times \cosh kh e^{-k(y+\eta-h)} J_0(ka)J_0(kR)dk, \quad (26)$$

$$\phi_2^{(1)} = 4\pi a \sin\sigma t \int_0^\infty \left\{ W_2^{(1)}(k,y) + \frac{X_2^{(1)}(k,y)}{m_1(k)\Delta(k)\cosh kh} \right\} J_0(kR)dk - 4\pi a \int_0^\infty \sigma\varepsilon k E(k)\left\{ F(\gamma_1,\gamma_2,\alpha)T(t,\alpha) - F(\gamma_1,\gamma_2,\beta)T(t,\beta) \right\} e^{k(h-\eta)} \cosh k(h-y) \times J_0(ka)J_0(kR)dk + 4\pi a \int_0^\infty \sigma a_1(k)E(k) \times \left\{ F(\rho_1,\rho_2,\alpha)T(t,\alpha) - F(\rho_1,\rho_2,\beta)T(t,\beta) \right\} \times e^{-k\eta} \sinh ky J_0(ka)J_0(kR)dk, \quad (27)$$

Where

$$T(t,v) = \frac{\sin vt}{v(v^2-\sigma^2)},$$

$$W_1^{(1)}(k,y) = \left[e^{-k|y-\eta|} - e^{-k(y+\eta)} \right] J_0(ka),$$

$$W_2^{(1)}(k,y) = e^{-k\eta}\sinh ky,$$

$$X_1^{(1)}(k,y) = \left[m_1(k)\Gamma_2(k) + a_1(k)\Gamma_3(k) \right] \times e^{-k(y+\eta-h)} J_0(ka),$$

$$X_2^{(1)}(k,y) = \left[m_1(k)\Gamma_2(k) + a_1(k)\Gamma_3(k) \right] e^{-k\eta} \times \sinh ky J_0(ka) + \left[m_1(k)\left\{ Kk\left(Dk^4+1\right) \right\} - a_1(k)\Gamma_3(k) \right] e^{k(h-\eta)} \cosh k(h-y) J_0(ka),$$

$$\Gamma_2(k) = k^2(1-s)\left(Dk^4+1-\varepsilon K\right)\sinh kh \cosh kh + KDk^5\left(\sinh^2 kh - s\cosh^2 kh\right) - Kk,$$

$$\Gamma_3(k) = K^2(ks\varepsilon+1)\cosh^2 kh + K^2(s+k\varepsilon) \times \sinh kh \cosh kh,$$

$$\Delta(k) \equiv Ks\left\{ k\left(Dk^4+1-\varepsilon K\right)\cosh kh - K\sinh kh \right\} - \left\{ k(1-s) - K \right\}\left\{ k\left(Dk^4+1-\varepsilon K\right)\sinh kh - K\cosh kh \right\}. \quad (28)$$

In order to find the expressions in the steady-state from the Eqs. (26) and (27), we now introduce Cauchy principal values at $k = \lambda_1, \lambda_2$ ($\lambda_1 < \lambda_2$) which are the only real positive roots of $\Delta(k) = 0$. Also, this dispersion equation has one negative real root and four complex roots in the four quadrants of the complex k-plane (cf. Das and Mandal (2007)). Hence as $t \to \infty$, using the Riemann Lebesgue lemma, we obtain

$$\phi_1^{(1)} = 2\pi a \sin\sigma t \int_0^\infty \left\{ W_1^{(1)}(k,y) - 2\frac{X_1^{(1)}(k,y)}{m_1(k)\Delta(k)} \right\} \times J_0(kR)dk - 4\pi^2 a\cos\sigma t\left\{ N_1^{(1)^+}(\lambda_1,y) J_0(\lambda_1 R) + N_1^{(1)^-}(\lambda_2,y)J_0(\lambda_2 R) \right\}, \quad (29)$$

$$\phi_2^{(1)} = 4\pi a \sin\sigma t \int_0^\infty \left\{ W_2^{(1)}(k,y) + \frac{X_2^{(1)}(k,y)}{m_1(k)\Delta(k)\cosh kh} \right\} J_0(KR)dk - 4\pi^2 a\cos\sigma t \times \left\{ N_2^{(1)^+}(\lambda_1,y)J_0(\lambda_1 R) + N_2^{(1)^-}(\lambda_2,y)J_0(\lambda_2 R) \right\}, \quad (30)$$

where

$$N_1^{(1)^\pm}(k,y) = \frac{P_1^{(1)^\pm}(k,y)}{H^\pm(k)} J_0(ka),$$

$$N_2^{(1)^\pm}(k,y) = \frac{Q_2^{(1)^\pm}(k,y)}{H^\pm(k)} J_0(ka),$$

$$L(k) = m_2^2 - 4m_1 m_3,$$

$$P_1^{(1)^\pm}(k,y) = \pm 2\left\{ \left(m_2 \pm \sqrt{L}\right)(a_2 m_1 - a_1 m_2) + 2m_1 m_3 (a_1 - m_1) \right\} \cosh kh e^{-k(y+\eta-h)},$$

$$H^\pm(k) = 2\sqrt{L}\left(m_1 m_2' - m_1' m_2\right) \pm \left(m_1 L' - 2m_1' L\right),$$

$$Q_2^{(1)^\pm}(k,y) = \pm 2\left[\left(m_2 \pm \sqrt{L}\right)\left\{ (b_2 m_1 - \varepsilon k m_2)e^{kh} \times \cosh k(h-y) - (a_2 m_1 - a_1 m_2)\sinh ky \right\} + 2m_3^2\left\{ \varepsilon k e^{kh}\cosh k(h-y) - (a_1 - m_1)\sinh ky \right\} \right] e^{-k\eta}.$$

In Eqs. (29) and (30) the integrals are in the sense of Cauchy principal value. Now to investigate the behavior of these integrals for large R, we put $2J_0(kR) = H_0^{(1)}(kR) + H_0^{(2)}(kR)$ and rotate the contour in the complex k-plane for the integral involving $H_0^{(1)}(kR)$ in the first quadrant and for the integral involving $H_0^{(2)}(kR)$ in the fourth quadrant. For large R one must include the residue terms at $k = \lambda_1$ and $k = \lambda_2$, because all other contributions to the integrals will be exponentially small. Thus as $R \to \infty$, we find

$$\phi_1^{(1)} = -4\pi^2 a\sqrt{\frac{2}{\pi\lambda_1 R}}\Big\{G_1^{(1)}(\lambda_1, y)\sin\sigma t \times\sin\left(\lambda_1 R - \frac{\pi}{4}\right) + N_1^{(1)^+}(\lambda_1, y)\cos\sigma t \times\cos\left(\lambda_1 R - \frac{\pi}{4}\right)\Big\} - 4\pi^2 as\sqrt{\frac{2}{\pi\lambda_2 R}} \times\Big\{G_1^{(1)}(\lambda_2, y)\sin\sigma t\sin\left(\lambda_2 R - \frac{\pi}{4}\right) + N_1^{(1)^-}(\lambda_2, y)\cos\sigma t\cos\left(\lambda_2 R - \frac{\pi}{4}\right)\Big\}, \tag{31}$$

$$\phi_2^{(1)} = -4\pi^2 a\sqrt{\frac{2}{\pi\lambda_1 R}}\Big\{G_2^{(1)}(\lambda_1, y)\sin\sigma t \times\sin\left(\lambda_1 R - \frac{\pi}{4}\right) + N_2^{(1)^+}(\lambda_1, y)\cos\sigma t \times\cos\left(\lambda_1 R - \frac{\pi}{4}\right)\Big\} - 4\pi^2 a\sqrt{\frac{2}{\pi\lambda_2 R}} \times\Big\{G_2^{(1)}(\lambda_2, y)\sin\sigma t\sin\left(\lambda_2 R - \frac{\pi}{4}\right) + N_2^{(1)^-}(\lambda_2, y)\cos\sigma t\cos\left(\lambda_2 R - \frac{\pi}{4}\right)\Big\}, \tag{32}$$

where

$$G_1^{(1)}(k, y) = \frac{-X_1^{(1)}(k, y)}{m_1(k)\Delta'(k)},$$

$$G_2^{(1)}(k, y) = \frac{X_2^{(1)}(k, y)}{m_1(k)\Delta'(k)\cosh kh}.$$

We expect that $G_j^{(1)}(\lambda_1, y) = N_j^{(1)^+}(\lambda_1, y)$ and $G_j^{(1)}(\lambda_2, y) = N_j^{(1)^-}(\lambda_2, y)(j = 1,2)$. It is difficult to prove analytically. However that these are the same can be shown numerically. For this purpose we present in Table 1 and Table 2 the numerical values of $G_j^{(1)}, N_j^{(1)^\pm}(j = 1,2)$ for a representative set of values of different parameters (e.g. $s = 0.4$ $\frac{\varepsilon}{h} = 0.01,\ \frac{D}{h^4} = 0.5,\ Kh = 1,\ \frac{\eta}{h} = 1.5,\ \frac{a}{h} = 0.2$ for which $\lambda_1 = 0.84$ and $\lambda_2 = 2.3463$) and a set of values of y. From these tables, it is obvious that $G_j^{(1)}(\lambda_1, y) = N_j^{(1)^+}(\lambda_1, y)$ and $G_j^{(1)}(\lambda_2, y) = N_j^{(1)^-}(\lambda_2, y)$. In fact for other values of the different parameters s, $\frac{\varepsilon}{h}$ etc. and y, the numerical values of $G_j^{(1)}$ and $N_j^{(1)^+}$ for surface wave mode λ_1 and $G_j^{(1)}$ and $N_j^{(1)^-}$ for interface wave mode λ_2 are seen to be the same.

Thus, in the far-field after a long time, the potentials $\phi_j^{(1)}$ behave as outgoing waves given by

$$\phi_1^{(1)} = -4\pi^2 a\sum_{i=1}^{2} qi\sqrt{\frac{2}{\pi\lambda_i R}}G_1^{(1)}(\lambda_i, y) \times\cos\left(\lambda_i R - \sigma t - \frac{\pi}{4}\right), \tag{33}$$

Table 1 Numerical values of $G_1^{(1)}(\lambda_1, y) = N_1^{(1)^+}(\lambda_1, y)$ for a set of of values of y

	λ1 = 0.84		λ2 = 2.3463	
y	$G_1^{(1)}$	$N_1^{(1)^+}$	$G_1^{(1)}$	$N_1^{(1)^-}$
1.1	0.0910	0.0910	0.3753	0.3753
1.3	0.0769	0.0769	0.2347	0.2347
1.5	0.0650	0.0650	0.1468	0.1468
1.7	0.0550	0.0550	0.0918	0.0918
1.9	0.0465	0.0465	0.0574	0.0574
2	0.0427	0.0427	0.0454	0.0454

Table 2 Numerical values of $G_2^{(1)}(\lambda_2, y) = N_2^{(1)^-}(\lambda_2, y)$ for a set of of values of y

	λ1 = 0.84		λ2 = 2.3463	
y	$G_2^{(1)}$	$N_2^{(1)^+}$	$G_2^{(1)}$	$N_2^{(1)^-}$
0.1	0.2416	0.2416	-0.0962	-0.0962
0.3	0.2061	0.2061	-0.1166	-0.1166
0.5	0.1765	0.1765	-0.1632	-0.1632
0.7	0.1518	0.1518	-0.2464	-0.2464
0.8	0.1411	0.1411	-0.3071	-0.3071
0.9	0.1314	0.1314	-0.3848	-0.3848

where $q_1 = 1$ and $q_2 = s$, and

$$\phi_2^{(1)} = -4\pi^2 a\sum_{i=1}^{2}\sqrt{\frac{2}{\pi\lambda_i R}}G_2^{(1)}(\lambda_i, y) \times\cos\left(\lambda_i R - \sigma t - \frac{\pi}{4}\right). \tag{34}$$

5. Ring Source Submerged In Upper Fluid

In this section we find the velocity potentials $\phi_j^{(2)}$ (j = 1,2) due to a ring source submerged in the upper fluid and examine its behavior at the steady-state at a large distance from the center of the ring.

A solution for $\Phi_j^{(2)}(R, y, p)$'s (j = 1,2) can be represented as

$$\Phi_1^{(2)} = \int_0^\infty A_1^{(2)}(k)e^{-k(y-h)}J_0(ka)J_0(kR)dk. \tag{35}$$

$$\Phi_2^{(2)} = M(p)\Big[\phi_0 - 2\pi a\int_0^\infty e^{-k(y+\eta)}J_0(ka) \times J_0(kR)dk\Big] + \int_0^\infty\Big\{B_2^{(2)}(k)\cosh k(h-y) + C_2^{(2)}(k)\sinh ky\Big\}\frac{J_0(ka)}{\cosh kh}J_0(kR)dk. \tag{36}$$

The functions $A_1^{(2)}(k), B_2^{(2)}(k), C_2^{(2)}(k)$ are unknown and are determined by using the conditions (13) − (15). These functions when substituted into the Eqs. (35) and (36) produce

$$\Phi_1^{(2)} = M(p)\Big[U_1^{(2)}(R,y) + 4\pi as\int_0^\infty c_1(k)E(k) \times\left\{\frac{F(\sigma_1,\sigma_2,\alpha)}{p^2+\alpha^2} - \frac{F(\sigma_1,\sigma_2,\beta)}{p^2+\beta^2}\right\}e^{-k(y-h)} \times J_0(ka)J_0(kR)dk\Big], \quad (37)$$

$$\Phi_2^{(2)} = M(p)\Big[U_2^{(2)}(R,y) + 4\pi a\int_0^\infty d_1(k)E(k) \times\left\{\frac{F(\delta_1,\delta_2,\alpha)}{p^2+\alpha^2} - \frac{F(\delta_1,\delta_2,\beta)}{p^2+\beta^2}\right\} \times\frac{\cosh k(h-y)}{\cosh kh}J_0(ka)J_0(kR)dk - 4\pi as\int_0^\infty c_1(k)E(k)\left\{\frac{F(\sigma_1,\sigma_2,\alpha)}{p^2+\alpha^2} - \frac{F(\sigma_1,\sigma_2,\beta)}{p^2+\beta^2}\right\}\frac{\sinh ky}{\cosh kh}J_0(ka)J_0(kR)dk\Big], \quad (38)$$

where

$$U_1^{(2)}(R,y) = 4\pi as\int_0^\infty \frac{c_1(k)}{m_1(k)}e^{-k(y-h)} \times J_0(ka)J_0(kR)dk,$$

$$U_2^{(2)}(R,y) = 2\pi a\int_0^\infty\left\{e^{-k|y-\eta|} - e^{-k(y+\eta)}\right\} \times J_0(ka)J_0(kR)dk + 4\pi a\int_0^\infty \frac{d_1(k)}{m_1(k)} \times\frac{\cosh k(h-y)}{\cosh kh}J_0(ka)J_0(kR)dk +4\pi a\int_0^\infty\left\{e^{-kh}\sinh k\eta - s\frac{c_1(k)}{m_1(k)}\right\} \times\frac{\sinh ky}{\cosh kh}J_0(ka)J_0(kR)dk,$$

$$c_1(k) = \cosh kh(\sinh k\eta + \varepsilon k\cosh k\eta),$$

$$c_2(k) = gk(Dk^4+1)\cosh kh\cosh k\eta,$$

$$d_1(k) = \varepsilon k\left\{\cosh k(h-\eta)(s\sinh kh + \cosh kh) - s\sinh k\eta\right\},$$

$$d_2(k) = gk\Big[(Dk^4+1)\left\{\cosh k(h-\eta)\big(s\sinh kh + \cosh kh\big) - s\sinh k\eta\right\} + \varepsilon k(1-s) \times\cosh kh\cosh k(h-\eta)\Big],$$

$$d_3(k) = (1-s)g^2k^2(Dk^4+1)\cosh kh\cosh k(h-\eta),$$

$$\sigma_1 = \frac{c_2m_1 - c_1m_2}{c_1m_1}, \quad \sigma_2 = \frac{m_3}{m_1},$$

$$\delta_1 = \frac{d_2m_1 - d_1m_2}{d_1m_1}, \quad \delta_2 = \frac{d_1m_3 - d_3m_1}{d_1m_1}.$$

To determine the potentials due to a source of time-harmonic strength, we take Laplace inversion of (37) and (38) and then substitute $m(t) = \sin\sigma t$. This yields

$$\phi_1^{(2)} = \sin\sigma t U_1^{(2)}(R,y) + 4\pi as\Big[\int_0^\infty c_1(k)E(k) \times\left\{F(\sigma_1,\sigma_2,\alpha)S(t,\alpha) - F(\sigma_1,\sigma_2,\beta)S(t,\beta)\right\} \times e^{-k(y-h)}J_0(ka)J_0(kR)dk\Big], \quad (39)$$

$$\phi_2^{(2)} = \sin\sigma t U_2^{(2)}(R,y) + 4\pi a\Big[\int_0^\infty d_1(k)E(k) \times\left\{F(\delta_1,\delta_2,\alpha)S(t,\alpha) - F(\delta_1,\delta_2,\beta)S(t,\beta)\right\} \times\frac{\cosh k(h-y)}{\cosh kh}J_0(ka)J_0(kR)dk\Big] - 4\pi as\Big[\int_0^\infty c_1(k)E(k)\left\{F(\sigma_1,\sigma_2,\alpha)S(t,\alpha) - F(\sigma_1,\sigma_2,\beta)S(t,\beta)\right\}\frac{\sinh ky}{\cosh kh} \times J_0(ka)J_0(kR)dk\Big]. \quad (40)$$

Using Riemann Lebesgue lemma and rotating the contour in an appropriate manner as has been done in section 4, we find that for large R and large t the potentials $\phi_j^{(2)}$'s (j = 1,2) have the following representations:

$$\phi_1^{(2)} = -4\pi^2 as\sqrt{\frac{2}{\pi\lambda_1 R}}\left\{G_1^{(2)}(\lambda_1,y)\sin\sigma t \times\sin(\lambda_1 R - \frac{\pi}{4}) + N_1^{(2)^+}(\lambda_1,y)\cos\sigma t \times\cos(\lambda_1 R - \frac{\pi}{4})\right\} - 4\pi^2 as\sqrt{\frac{2}{\pi\lambda_2 R}}\left\{G_1^{(2)}(\lambda_2,y) \times\sin\sigma t\sin(\lambda_2 R - \frac{\pi}{4}) + N_1^{(2)^-}(\lambda_2,y)\cos\sigma t \times\cos(\lambda_2 R - \frac{\pi}{4})\right\}, \quad (41)$$

$$\phi_2^{(2)} = -4\pi^2 a\sqrt{\frac{2}{\pi\lambda_1 R}}\left\{G_2^{(2)}(\lambda_1,y)\sin\sigma t \times\sin(\lambda_1 R - \frac{\pi}{4}) + N_2^{(2)^+}(\lambda_1,y)\cos\sigma t \times\cos(\lambda_1 R - \frac{\pi}{4})\right\} - 4\pi^2 a\sqrt{\frac{2}{\pi\lambda_2 R}}\left\{G_2^{(2)}(\lambda_2,y) \times\sin\sigma t\sin(\lambda_2 R - \frac{\pi}{4}) + N_2^{(2)^-}(\lambda_2,y)\cos\sigma t \times\cos(\lambda_2 R - \frac{\pi}{4})\right\}, \quad (42)$$

where

$$N_1^{(2)^\pm}(k,y) = \frac{P_1^{(2)^\pm}(k,y)}{H^\pm(k)} J_0(ka),$$

$$N_2^{(2)^\pm}(k,y) = \frac{Q_2^{(2)^\pm}(k,y)}{H^\pm(k)} J_0(ka),$$

$$P_1^{(2)^\pm}(k,y) = \pm 2\left\{(m_2 \pm \sqrt{L})(c_2 m_1 - c_1 m_2) + 2c_1 m_1 m_3\right\} e^{-k(y-h)},$$

$$Q_2^{(2)^\pm}(k,y) = \pm 2\Big[(m_2 \pm \sqrt{L})\{(d_2 m_1 - d_1 m_2) \times \cosh k(h-y) - s(c_2 m_1 - c_1 m_2)\sinh ky\} + 2m_3\{(d_1 m_3 - d_3 m_1)\cosh k(h-y) - sc_1 m_3 \sinh ky\}\Big],$$

$$G_1^{(2)}(k,y) = \frac{X_1^{(2)}(k,y)}{\Delta'(k)},$$

$$G_2^{(2)}(k,y) = \frac{X_2^{(2)}(k,y)}{m_1(k)\Delta'(k)\cosh kh},$$

$$X_1^{(2)}(k,y) = \Gamma_4(k) e^{-k(y-h)} J_0(ka),$$

$$X_2^{(2)}(k,y) = -sm_1(k)\Gamma_4(k)\sinh ky J_0(ka) + \Big[\{\Gamma_5(k)(Ks\cosh kh - k\sinh kh + ks\sinh kh + K\sinh kh) - K^2\Gamma_6(k)\} \times d_1(k) - k(1-s)\Gamma_5(k)\Gamma_6(k)\cosh kh \times \cosh k(h-\eta) - k^2\varepsilon s(1-s)\Gamma_5(k)\cosh kh \times \cosh k\eta + Kk(Dk^4+1)\Gamma_6(k)\{\Gamma_6(k) \times \cosh k(h-\eta) - s\sinh k\eta\}\Big]\cosh k(h-y)\, J_0(ka),$$

$$\Gamma_4(k) = K\{-K\sinh k\eta + \Gamma_5(k)\cosh k\eta\},$$

$$\Gamma_5(k) = k(Dk^4 + 1 - \varepsilon K),$$

$$\Gamma_6(k) = (s\sinh kh + \cosh kh).$$

As in section 4, here also, it can be shown numerically that $G_j^{(2)}(\lambda_1,y) = N_j^{(2)^+}(\lambda_1,y)$ and $G_j^{(2)}(\lambda_2,y) = N_j^{(2)^-}(\lambda_2,y)(j=1,2)$.

Thus, in the far-field after a long time, the potentials $\phi_j^{(2)}$ behave as outgoing waves given by

$$\phi_1^{(2)} = -4\pi^2 as\sum_{i=1}^{2}\sqrt{\frac{2}{\pi\lambda_i R}}G_1^{(2)}(\lambda_i,y) \times\cos(\lambda_i R - \sigma t - \frac{\pi}{4}), \tag{43}$$

$$\phi_2^{(2)} = -4\pi^2 a\sum_{i=1}^{2}\sqrt{\frac{2}{\pi\lambda_i R}}G_2^{(2)}(\lambda_i,y) \times\cos(\lambda_i R - \sigma t - \frac{\pi}{4}). \tag{44}$$

6. SURFACE WAVES AND INTERFACE WAVES

In this section we present the upper surface profile and the interface profile at the steady-state. For this, we observe that the displacements at these surfaces are related to the potential functions as

$$\frac{\zeta_2^{(i)}}{h}(R,t) = \frac{1}{h}\mathrm{Re}\left\{\frac{g^2}{\sigma^3}\int_0^t \frac{\partial}{\partial y}\phi_2^{(i)}(R,0,\tau)d\tau\right\},$$
$$\frac{\zeta_1^{(i)}}{h}(R,t) = \frac{1}{h}\mathrm{Re}\left\{\frac{g^2}{\sigma^3}\int_0^t \frac{\partial}{\partial y}\phi_1^{(i)}(R,h,\tau)d\tau\right\} \tag{45}$$

When the ring source is submerged in the lower fluid, Fig. 1 depicts the surface displacement and the interface displacement for the surface wave mode and the interface wave mode against $\frac{R}{h}$ for fixed s = 0.4 $\frac{\varepsilon}{h} = 0.01$, $\frac{\eta}{h} = 1.5$, $\frac{a}{h} = 0.2$, $\frac{D}{h^4} = 0.01$, $Kh = 1$, $\sigma t = 50$. From these figures we notice that for the surface wave mode, the amplitude of the surface waves is greater than that of the interface waves, and both the surface and interface waves are in phase. On the contrary, for the interface wave mode, the amplitude of the surface waves is smaller than that of the interface waves, and the surface and interface waves are 180° out of the phase. When ring source is submerged in the upper fluid, Fig. 2 depicts the surface displacement and interface displacement for the surface wave mode and the interface wave mode against $\frac{R}{h}$ for fixed s = 0.4, $\frac{\varepsilon}{h} = 0.01$, $\frac{\eta}{h} = 0.5$, $\frac{a}{h} = 0.2$, $\frac{D}{h^4} = 0.01$, $Kh = 1$, $\sigma t = 50$. The curves are somewhat similar to those for ring source submerged in lower fluid and dis-play the same characteristics.

To display the effect of the flexural rigidity of the elastic plate on the wave motion generated due to the presence of a ring source in the lower fluid, the dimensionless interface displacement $\frac{\zeta_1^{(1)}}{h}$ and the surface displacement $\frac{\zeta_2^{(1)}}{h}$ for surface wave mode and interface wave mode are presented graphically against $\frac{R}{h}$ in Figs. 3 and 4 respectively. For plotting all the graphs in these two figures we choose s = 0.4, $\frac{\varepsilon}{h} = 0.01$, $\frac{\eta}{h} = 1.5$, $\frac{a}{h} = 0.2$, $Kh = 1$, $\sigma t = 50$ and vary $\frac{D}{h^4}$ as $\frac{D}{h^4}$ = 2,1,0.5. It is observed from Fig. 3 that for surface wave mode, the wave amplitude of the interface wave increases with the decreasing values of $\frac{D}{h^4}$. However, for interface wave mode, no variation in the interface wave profile is noticed. This is in contrast to the surface wave profile where the amplitude of the surface wave is seen to increase with the decreasing values of $\frac{D}{h^4}$ irrespective of surface / interface wave modes (see Fig. 4).

To analyze the effect of the flexural rigidity of the elastic plate on the wave motion generated due to the presence of a ring source in the upper fluid, the dimensionless interface displacement $\frac{\zeta_1^{(2)}}{h}$ and surface displacement $\frac{\zeta_2^{(2)}}{h}$ for surface wave mode and interface wave mode are presented graphically in Figs. 5 and 6. The graphs in these figures display the same characteristics as those in Figs. 3 and 4. Wave amplitudes of the surface and the interface waves for the surface wave mode due to a ring source placed in the upper fluid are slightly large compared to those generated by the source when it is situated in the lower fluid. On the contrary, for the interface wave mode, the amplitudes of the surface and the interface waves due to a ring source in upper fluid are less than those due to a ring source placed in the lower fluid.

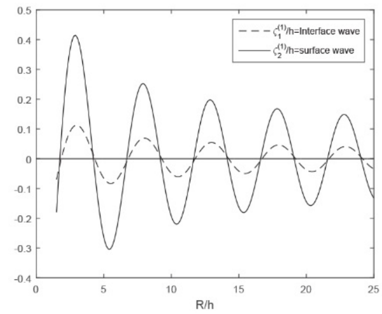

(a) Surface wave mode

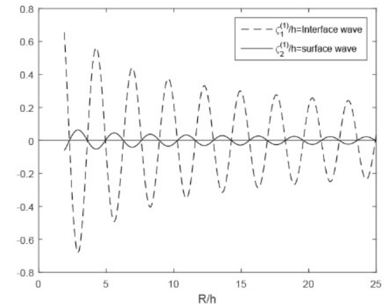

(b) Interface wave mode

Fig. 1. Ring source submerged in lower fluid: surface wave $(\zeta_2^{(1)}/h)$ and interface wave $(\zeta_1^{(1)}/h)$ against *R/h* for fixed *s* = 0.4 $\frac{\varepsilon}{h}=0.01,\ \frac{\eta}{h}=1.5,\ \frac{a}{h}=0.2, \frac{D}{h^4}=0.01,\ Kh=1,$ $\sigma t=50.$

7. CONCLUSION

The velocity potentials due to a submerged horizontal ring of wave sources of time-dependent strength present in either of the fluids of a two-fluid medium are obtained when the upper layer is of finite height above the mean interface and bounded by a thin

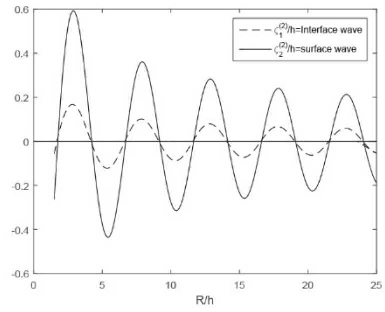

(a) Surface wave mode

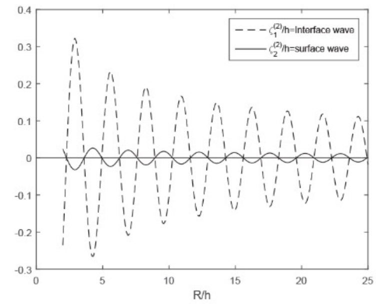

(b) Interface wave mode

Fig. 2. Ring source submerged in upper fluid: surface wave $(\zeta_2^{(2)}/h)$ and interface wave $(\zeta_1^{(2)}/h)$ against R/h for fixed s = 0.4, $\frac{\varepsilon}{h}=0.01,\ \frac{\eta}{h}=0.5,\ \frac{a}{h}=0.2,\ \frac{D}{h^4}=0.01,\ Kh=1,$ $\sigma t=50.$

elastic plate modeling a thin floating sheet of ice, while the lower layer extends infinitely downwards. The asymptotic representations of the wave motions for large time and large distance are derived for the case when the ring source is placed in the lower layer and also when it is placed in the upper layer. In these asymptotic representations, the two different coefficients for surface wave mode produce almost the same numerical results although it is difficult to prove their equivalence analytically. The same comment applies to the two different coefficients for interface wave mode. This shows that in the steady-state analysis, the potentials provide the existence of outgoing progressive waves. The dimensionless surface and interface wave displacements are depicted graphically for both the wave modes. It has been observed that for the surface wave mode, the amplitude of the surface waves is greater than that of the interface waves, and both the surface and interface waves are in phase. On the contrary, for the interface wave mode, the amplitude of the surface waves is

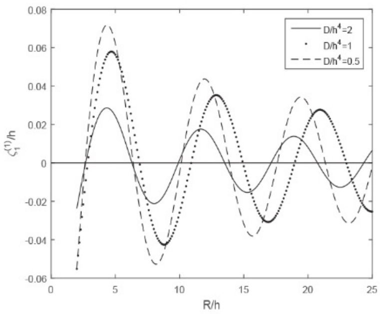

(a) Surface wave mode

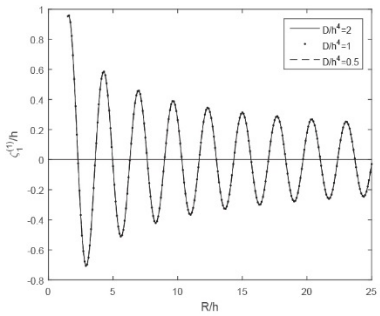

(b) Interface wave mode

Fig. 3. Ring source submerged in lower fluid: plot of interface wave $(\zeta_1^{(1)}/h)$ against R/h for fixed s = 0.4, $\frac{\varepsilon}{h}=0.01,\ \frac{\eta}{h}=1.5,\ \frac{a}{h}=0.2,\ Kh=1,\ \sigma t=50.$

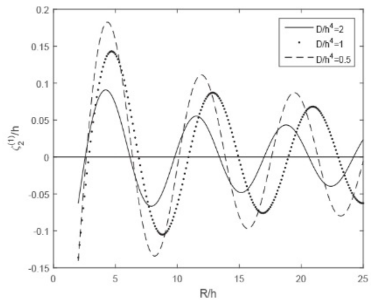

(a) Surface wave mode

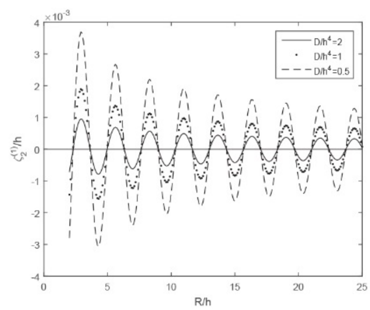

(b) Interface wave mode

Fig. 4. Ring source submerged in lower fluid: plot of surface wave $(\zeta_2^{(1)}/h)$ against *R/h* for fixed s = 0.4, $\frac{\varepsilon}{h}=0.01,\ \frac{\eta}{h}=1.5,\ \frac{a}{h}=0.2,\ Kh=1,\ \sigma t=50.$

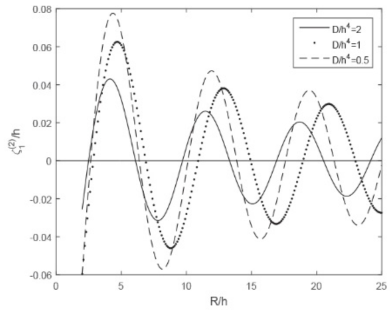

(a) Surface wave mode

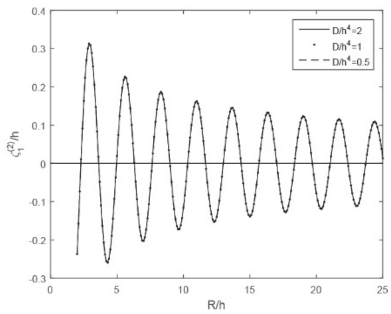

(b) Interface wave mode

Fig. 5. Ring source submerged in upper fluid: plot of interface wave $(\zeta_1^{(2)}/h)$ against *R/h* for fixed s = 0.4, $\frac{\varepsilon}{h}=0.01,\ \frac{\eta}{h}=0.5,\ \frac{a}{h}=0.2,\ Kh=1,\ \sigma t=50.$

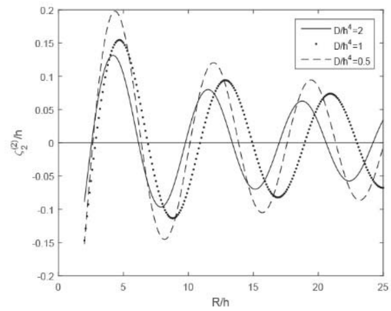

(a) Surface wave mode

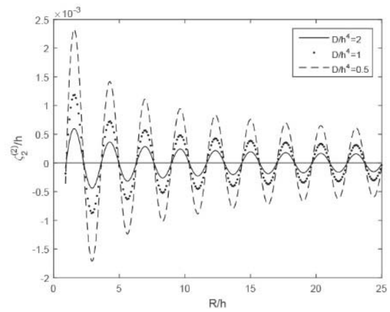

(b) Interface wave mode

Fig. 6. Ring source submerged in upper fluid: plot of surface wave $(\zeta_2^{(2)}/h)$ against *R/h* for fixed s = 0.4, $\frac{\varepsilon}{h}=0.01,\ \frac{\eta}{h}=0.5,\ \frac{a}{h}=0.2,\ Kh=1,\ \sigma t=50.$

smaller than that of the interface waves, and the surface and interface waves are 180° out of phase. Surface and interface waves are presented graphically for different values of the flexural rigidity of the elastic plate for both the wave modes. It is observed that for surface wave mode the wave amplitudes of the surface and interface waves increase with the decreasing values of $\frac{D}{h^4}$ and for interface wave mode the wave amplitudes of the interface waves are the same but the amplitude of the surface wave increases with the decreasing values of $\frac{D}{h^4}$.

REFERENCES

Das, D. and B. N. Mandal (2007). Wave scattering by a horizontal circular cylinder in a two-layer fluid with an ice-cover. International Journal of Engineering Science 45(10), 842–872.

Feng, X. and D. Q. Lu (2009). An optimization of eigenfunction expansion method for the interaction of water waves with an elastic plate. Journal of Hydrodynamics, Ser. B 21(4), 526–530.

Fenton, J. D. (1978). Wave forces on vertical bodies of revolution. *Journal of Fluid Mechanics* 85(2), 241–255.

Fox, C. and V. A. Squire (1994). On the oblique reflexion and transmission of ocean waves at shore fast sea ice. Philosophical Transactions of the Royal Society of London A: Mathematical, *Physical and Engineering Sciences* 347(1682), 185–218.

Gayen, R. and B. N. Mandal (2004). Motion due to ring source in ice-covered water. *International Journal of Engineering Science* 42, 1645–1654.

Gayen, R. and B. N. Mandal (2006). Motion due to fundamental singularities in finite depth water with an elastic solid cover. Fluid Dynamics Research 38(4), 224–240.

Gorgui, M. A. and S. E. Kassem (1978). Basic singularities in the theory of internal wave. *The Quarterly Journal of Mechanics and Applied Mathematics* 31(1), 31–48.

Hulme, A. (1981). The potential of a horizontal ring of wave sources in a fluid with a free surface. Proceedings of the Royal Society of London A: Mathematical, *Physical and Engineering Sciences* 375(1761), 295–305.

Lu, D. Q. and S. Q. Dai (2008). Flexural-and capillary-gravity waves due to fundamental singularities in an inviscid fluid of finite depth. *International Journal of Engineering Science* 46(11), 1183–1193.

Mandal, B. N. and K. Kundu (1987). Ring source potentials in a fluid with an inertial surface in the presence of surface tension. *International Journal of Engineering Science* 25(11-12), 1383–1386.

Mandal, B. N. and K. Kundu (1988). Ring source potentials in two superposed fluids separated by an inertial surface. *International Journal of Mathematics and Mathematical Sciences* 11(3), 535–541.

Mandal, B. N. and R. N. Chakrabarti (1995). Potential due to a horizontal ring of wave sources in a two-fluid medium. *Proceedings of the Indian National Science Academy* 61, 433–439.

Manyanga, D. and W. Duan (2011). Green functions with pulsating sources in a two-layer fluid of finite depth. China Ocean Engineering 25(4), 609–624.

Mohapatra, S. and S. N. Bora (2012). Exciting forces due to interaction of water waves with a submerged sphere in an ice-covered two-layer fluid of finite depth. *Applied Ocean Research* 34, 187–197.

Panda, S. and S. C. Martha (2013). Interaction of water waves with small undulations on a porous bed in a two-layer ice-covered fluid. *Journal of Marine Science and Application* 12(4), 381–392.

Rhodes-Robinson, P. F. (1984). On the generation of water waves at an inertial surface. *The Journal of the Australian Mathematical Society. Series B. Applied Mathematics* 25(03), 366–383.

Squire, V. A. and T. D. Williams (2008). Wave propagation across sea-ice thickness changes. Ocean Modelling 21(1), 1–11.

Ten, I. and M. Kashiwagi (2004). Hydrodynamics of a body floating in a two-layer fluid of finite depth, part 1: radiation problem. *Journal of Marine Science and Technology* 9(3), 127–141.

Thorne, R. C. (1953). Multipole expansions in the theory of surface waves. *Mathematical Proceedings of the Cambridge Philosophical Society* 49(04), 707–716.

Yeung, R. and T. Nguyen (1999). Waves generated by a moving source in a two-layer ocean of finite depth. *Journal of Engineering Mathematics* 35(1), 85–107.